Continent-Ocean Chemical Heterogeneity in the Mantle Based on Seismic Tomography

Alessandro M. Forte,* Adam M. Dziewonski, Richard J. O'Connell

Seismic models of global-scale lateral heterogeneity in the mantle show systematic differences below continents and oceans that are too large to be purely thermal in origin. An inversion of the geoid, based on a seismic model that includes viscous flow in the mantle, indicates that the differences beneath continents and oceans can be accounted for by differences in composition in the upper mantle superposed on mantle-wide thermal heterogeneities. The net continent-ocean density differences, integrated over depth, are small and cause only a low flux of mass and heat across the asthenosphere and mantle transition zone.

Recent geodynamic interpretations (*1–5*) of global-scale heterogeneity in the seismic velocity of the mantle (*6–9*) have assumed a scaling coefficient, directly relating density perturbations to seismic velocity perturbations, that varies only with depth. This assumption should not hold if there are significant lateral variations in chemical composition, in which case this scaling coefficient may also vary laterally, with negative values possible (unlike purely thermal heterogeneity that is characterized by only positive values). It has been hypothesized that the growth and accretion of the continental crust will result in a subcontinental mantle that is chemically distinct from the suboceanic mantle (*10–12*). Here we use a model of a viscous (flowing) mantle, based on a recent seismic inference (6) of three-dimensional mantle structure, to infer the presence and magnitude of such continent-ocean chemical differences. The flow-induced perturbations in surface gravity (expressed here as geoid anomalies) that are predicted on the basis of the seismic heterogeneity are adjusted to fit the observed geoid anomalies. We thus infer the density-velocity scaling coefficients for the seismically inferred mantle heterogeneity that are, respectively, correlated and uncorrelated to the surface distribution of continents and oceans. Differences between these two scaling coefficients are used to infer the presence of chemically distinct continent-ocean heterogeneity. We also evaluate the impact of this chemical heterogeneity on the buoyancy-induced flow in the mantle.

To quantify the continent-ocean heterogeneity in the mantle, we considered a function that was defined to be 1 in all continental regions and to be 0 in all oceanic regions, and from which we subtracted its global average ($\approx 1/3$). We performed a least squares fit of this continent-ocean function to the relative shear-velocity perturbations $\delta v_S/v_S$ described by the seismic heterogeneity model SH8/U4L8 (6). We thereby obtained two complementary shear-velocity models: One model [called "correlated" and denoted by $(\delta v_S/v_S)_{co}$] is perfectly correlated with the continent-ocean function at all depths, and the second model [called "uncorrelated" (thermal) and denoted by $(\delta v_S/v_S)_{th}$] is completely uncorrelated with the continent-ocean function (Fig. 1A). Any difference in the chemical composition of the average subcontinental mantle from that of the suboceanic mantle will be embedded in the correlated seismic model. If this is the dominant form of upper-mantle chemical heterogeneity, we expect that the uncorrelated seismic model will then represent the portion of mantle heterogeneity that is primarily, if not wholely, thermal in origin.

The observed nonhydrostatic geoid (*13*) is directly dependent on the lateral variations of density in Earth's interior, and it is thus used to infer the density perturbations related to the correlated and uncorrelated seismic models. We partitioned the nonhydrostatic geoid into two parts that are, respectively, correlated and uncorrelated with the continent-ocean function. The root mean square (rms) amplitudes of the correlated and uncorrelated parts of the geoid, in the degree range $\ell = 2$ to 8, are, respectively, 11.5 m and 39.2 m. The continent-ocean signal in the long-wavelength geoid is not negligible (*14*), and it is anticorrelated with the small signal expected (*15*) from the isostatic compensation of density differences between the oceanic and continental crust. The origin of this continent-ocean geoid should therefore lie in the density heterogeneity in the mantle correlated to the continent-ocean function.

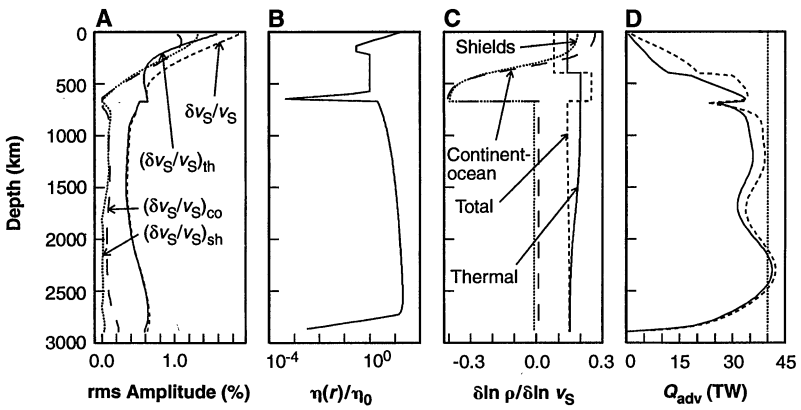

Fig. 1. (**A**) The rms amplitude of relative perturbations in seismic shear velocity. The short-dashed line represents the rms amplitude in model SH8/U4L8 (*6*). The long-dashed line and the solid line represent the rms amplitude of the heterogeneity in models $(\delta v_S/v_S)_{co}$ and $(\delta v_S/v_S)_{th}$ that are, respectively, correlated and uncorrelated with the continent-ocean function. The dotted line represents the rms amplitude of the model $(\delta v_S/v_S)_{sh}$ that is correlated to the zero-mean shield function. (**B**) A radial profile of relative viscosity in the mantle. The reference viscosity η_0 is not constrained by the geoid data. (**C**) The ratio between perturbations of density and seismic velocity ($\delta\ln\rho/\delta\ln v_S$) determined by inverting the nonhydrostatic geoid data in the context of a viscous flow model that uses the viscosity profile in (B). The short-dashed line represents the inferred ratio when all the heterogeneity in model SH8/U4L8 is considered. The long-dashed line and the solid line represent, respectively, the inferred ratios for the heterogeneity in models $(\delta v_S/v_S)_{co}$ and $(\delta v_S/v_S)_{th}$. The dotted line represents the ratio inferred for the seismic heterogeneity in model $(\delta v_S/v_S)_{sh}$. (**D**) The total vertical advection of heat Q_{adv} as a function of depth. The solid line is the prediction obtained when the heterogeneity in models $(\delta v_S/v_S)_{co}$ and $(\delta v_S/v_S)_{th}$ are separately converted to density heterogeneity according to the long-dashed and solid lines in (C). The dashed line is the prediction obtained when all of the heterogeneity in model SH8/U4L8 is treated as thermal, according to the solid line in (C). The advected heat flow is inversely proportional to the reference viscosity η_0. The value used here is $\eta_0 = 10^{21}$ Pa·s. The vertical dotted line represents the total heat flux observed at Earth's surface. Units are terawatts (10^{12} W).

A. M. Forte, Département de Sismologie, Institut de Physique du Globe de Paris, 4 place Jussieu, 75252 Paris Cedex 05, France.
A. M. Dziewonski and R. J. O'Connell, Department of Earth and Planetary Sciences, Harvard University, Cambridge, MA 02138, USA.
*To whom correspondence should be addressed.

The relation between the nonhydrostatic geoid and the mantle density heterogeneity is explained with a viscous flow model of the mantle (*16–19*). The viscous flow model we used (Fig. 1B) (*19*) assumes a compressible mantle in which there is a finite mass flux ("whole-mantle flow") between the upper and lower mantle. We obtained the density perturbations that drive the large-scale mantle flow by converting the seismic velocity perturbations in model SH8/U4L8, using a density-velocity scaling coefficient $\delta\ln\rho/\delta\ln v_S$ that we estimated from the nonhydrostatic geoid data. We assumed that $\delta\ln\rho/\delta\ln v_S$ is constant in the top 400 km, is constant in the transition zone (depth, 400 to 670 km), and varies smoothly in the lower mantle, and we applied the same geoid-inferred scaling coefficient (the short-dashed line in Fig. 1C) to both the correlated and uncorrelated seismic models.

We then obtained density-velocity scalings (Fig. 1C) for the uncorrelated seismic model [denoted by $(\delta\ln\rho/\delta\ln v_S)_{th}$] and for the correlated seismic model [denoted by $(\delta\ln\rho/\delta\ln v_S)_{co}$] by performing a single inversion of the geoid data in which we simultaneously solve for $(\delta\ln\rho/\delta\ln v_S)_{th}$ and $(\delta\ln\rho/\delta\ln v_S)_{co}$ (*20*). The depth variation of the uncorrelated scaling coefficient is similar to that recently proposed by Karato (*21*), and it thus appears that the heterogeneity in the uncorrelated seismic model is largely due to lateral temperature variations. In contrast, the depth variation of the correlated scaling coefficient is notably different. We have used other mantle viscosity profiles, such as that derived by King and Masters (*2*), and we found by using these profiles that the correlated scaling coefficient is characterized by positive values at shallow depths and negative values at greater depths, in the transition zone.

The models with separate (correlated and uncorrelated) scaling coefficients yield a 76% variance reduction to the long-wavelength geoid data, compared to a 65% variance reduction obtained on the basis of the single scaling coefficient (the short-dashed line in Fig. 1C). This improvement reflects the increased amplitude of the harmonic coefficient $C_{2,0}$, which describes the ellipticity of the predicted geoid (predicted = −23.5 m; observed = −27.6 m). Failure to fit this coefficient accounted for a large part of the misfit of previous models (*1*), and hence this result seems to resolve previous difficulties (*1*, *22*) in accounting for the observed dynamic ellipticity of Earth.

Precambrian shields are the oldest stable nuclei of continents, and it is thus possible that upper-mantle chemical heterogeneity, accumulated over the history of continental growth, may be strongest beneath the shields. We investigated this possibility by using a function defined to be 1 in all 5° by 5° surface cells corresponding to Precambrian shields and platforms in model GTR1 (*23*) and 0 in all other cells. We calculated the spherical harmonic decomposition of this field and removed its global average. We then partitioned the seismic heterogeneity into two orthogonal portions that are respectively correlated and uncorrelated with this zero-average shield function (Fig. 1A). The geoid-inferred density-velocity scaling coefficient for the heterogeneity correlated to the shield function shows nearly the same reversal in the depth variation of the scaling coefficient as in the case of the continent-ocean heterogeneity (Fig. 1C). This result shows that, in the long-wavelength analysis considered here, the difference between a description of chemical heterogeneity in terms of a shield function or a continent-ocean function is not important.

The change in sign of the correlated scaling coefficient, near a depth of 250 km, implies that continental roots are denser than average suboceanic mantle at shallow depths, whereas they become less dense than the suboceanic mantle at greater depths. This reversal over depth should produce an internal cancellation of the buoyancy forces created by the density difference between subcontinental and suboceanic mantle. If we assume that the continent-ocean heterogeneity is purely thermal in origin, the continent-ocean density contrasts given by $(\delta\ln\rho/\delta\ln v_S)_{th} \times (\delta v_S/v_S)_{co}$ will generate considerable downward flow beneath the continents (Fig. 2A). If we instead consider the continent-ocean density heterogeneity delivered by the correlated scaling coefficient, the vertical flow is much smaller (Fig. 2B). Thus, the continent-ocean heterogeneity is stabilized by the reversal of buoyancy with depth. This density heterogeneity does exert, however, a net vertical load on the surface and thereby produces a surface topography contribution (*24*) that is depressed in continental regions and elevated in oceanic regions. The magnitude of the flow-induced topography due to the uncorrelated (purely thermal) heterogeneity is substantially less (*24*) than the prediction of models without chemical heterogeneity (*5*).

Although the continent-ocean density heterogeneity is in quasi-isostatic equilibrium, this does not imply that all flow in the upper mantle vanishes. The presumably thermal heterogeneity $(\delta v_S/v_S)_{th}$, unrelated to continent-ocean differences, produces flow throughout the mantle. A comparison of Figs. 2C and 2D shows that the stabilization of continent-ocean density contrasts does lead to an appreciable reduction of the total vertical flow velocity beneath continents. However, as is evident in Fig. 2D, there remains a considerable amount of up-

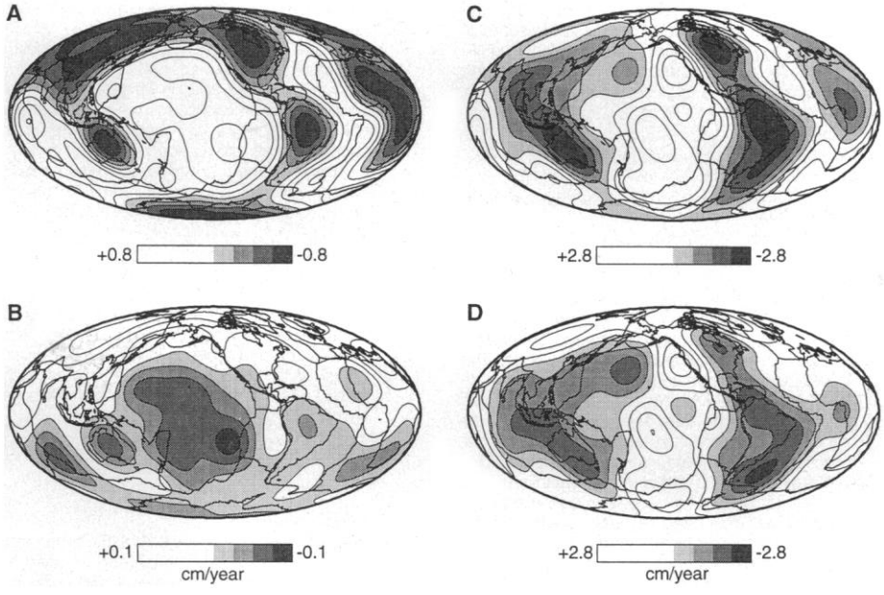

Fig. 2. Vertical flow velocities at a depth of 250 km predicted with a viscous flow model that uses the viscosity profile in Fig. 1B and $\eta_0 = 10^{21}$ Pa·s. (**A**) The vertical flow driven by continent-ocean heterogeneity, converted to density heterogeneity using the density-velocity scaling given by the solid line in Fig. 1C. (**B**) The vertical flow driven by continent-ocean heterogeneity, converted to density heterogeneity by using the density-velocity scaling given by the long-dashed line in Fig. 1C. (**C**) The vertical flow predicted when all the seismic heterogeneity in model SH8/U4L8 is converted to density heterogeneity by using the density-velocity scaling given by the solid line in Fig. 1C. (**D**) The vertical flow predicted when the seismic heterogeneity in models $(\delta v_S/v_S)_{co}$ and $(\delta v_S/v_S)_{th}$ are separately converted to density heterogeneity by using the density-velocity scaling given, respectively, by the long-dashed and solid lines in Fig. 1C. In all maps the velocity scale is in centimeters per year; shaded and unshaded areas represent, respectively, downward and upward flow.

per-mantle flow associated with the uncorrelated (thermal) heterogeneity $(\delta v_S/v_S)_{th}$.

The internal stability of the continent-ocean heterogeneity should have a significant impact on the vertical advection of heat throughout the upper mantle. The total advection of heat across any depth, calculated on the basis of the seismically inferred heterogeneity, is given by

$$Q_{adv}(r) = -\frac{r^2 c_p \rho_o(r)}{\alpha(r)}\left(\frac{\delta \ln \rho}{\delta \ln v_S}\right)_{th}(r)$$

$$\oint_{S_1} \frac{\delta v_S}{v_S}(r,\vartheta,\varphi) u_r(r,\vartheta,\varphi) dS$$

where S_1 denotes integration over the area of a unit sphere, c_p is the specific heat capacity at constant pressure, $\rho_o(r)$ is the radial density profile of the mantle, $\alpha(r)$ is the coefficient of thermal expansion, and u_r is the vertical flow velocity. We use the depth variation of thermal expansion $\alpha(r)$ from (*25*) and the Dulong-Petit limit c_p = 1260 J kg^{-1} K^{-1}. We then calculated u_r, and the resulting depth variation of advected heat, on the basis of the sum of the separate density contributions from the correlated and uncorrelated seismic models (the solid line in Fig. 1D). The heat advection we predicted (the dashed line in Fig. 1D) by assuming that all of the mantle heterogeneity is thermal in origin [u_r is calculated with the total density heterogeneity given by $(\delta \ln \rho/\delta \ln v_S)_{th} \times \delta v_S/v_S$] is significantly greater in the upper mantle than the heat advection predicted with the quasi-isostatic continent-ocean density heterogeneity. If the heat produced in the mantle by radioactive sources or secular cooling is substantial, then the advected heat flow should decrease with depth (unlike the relatively constant curve in Fig. 1D). In this case, the advected heat predictions in Fig. 1D would indicate that modifications to viscosity, thermal expansion, or $\delta \ln \rho/\delta \ln v_S$ may be needed.

Our analysis of continent-ocean heterogeneity in a viscous mantle suggests that it is supported in quasi-isostatic equilibrium because of the sign reversal in the geoid-inferred profile of the correlated density-velocity scaling coefficient. We interpret this result as indicating that any chemically induced density deficit in continental roots is overwhelmed at shallow depths by the thermally induced density increase due to their colder temperatures (*26*). At greater depths, the decrease in the temperature contrast between suboceanic and subcontinental mantle allows the chemical signal to appear.

REFERENCES AND NOTES

1. A. M. Forte, A. M. Dziewonski, R. L. Woodward, in *Dynamics of the Earth's Deep Interior and Earth Rotation*, J.-L. Le Mouël, D. E. Smylie, T. Herring, Eds. (AGU volume 72, American Geophysical Union, Washington, DC, 1993), pp. 135–166.
2. S. King and G. Masters, *Geophys. Res. Lett.* **19**, 1551 (1992).
3. M. G. Kogan and M. K. McNutt, *Science* **259**, 473 (1993).
4. J. P. Morgan and P. M. Shearer, *Nature* **365**, 506 (1993).
5. A. M. Forte, W. R. Peltier, A. M. Dziewonski, R. L. Woodward, *Geophys. Res. Lett.* **20**, 225 (1993).
6. A. M. Dziewonski and R. L. Woodward, *Acoust. Imag.* **19**, 785 (1992).
7. G. Masters, H. Bolton, P. Shearer, *Eos* (Spring Meeting Suppl.) **73**, 201 (1992).
8. R. L. Woodward, A. M. Forte, W.-J. Su, A. M. Dziewonski, in *Evolution of the Earth and Planets*, E. Takahashi, R. Jeanloz, D. Rubie, Eds. (AGU volume 74, American Geophysical Union, Washington, DC, 1993), pp. 89–109.
9. W.-J. Su, R. L. Woodward, A. M. Dziewonski, *J. Geophys. Res.* **99**, 6945 (1994).
10. G. J. F. MacDonald, *Rev. Geophys.* **1**, 587 (1963).
11. T. H. Jordan, *ibid.* **13**, 1 (1975).
12. ———, *Nature* **274**, 544 (1978).
13. We use the satellite-observed geoid field derived from the GEM-T2 model [J. G. Marsh *et al.*, *J. Geophys. Res.* **95**, 22043 (1990)] from which we first remove the hydrostatic rotational flattening [S. M. Nakiboglu, *Phys. Earth Planet. Inter.* **28**, 302 (1982)]. Because the seismic model SH8/U4L8 (*6*) describes lateral heterogeneity up to spherical harmonic degree ℓ = 8, we considered the nonhydrostatic geoid in the degree range ℓ = 2 to 8.
14. The amplitude of the continent-ocean geoid that we inferred is directly proportional to the coefficient measuring the cross-correlation between the long-wavelength (ℓ = 2 to 8) nonhydrostatic geoid and continent-ocean function (measured cross-correlation = −0.28). A common procedure is to estimate significance levels of the correlation coefficient by assuming that the harmonic coefficients of the two fields are (zero-mean) random samples from a bivariate normal distribution [R. J. O'Connell, *Geophys. J. R. Astron. Soc.* **23**, 299 (1971)]. The hypothesis that the measured cross-correlation of −0.28 (for 75 degrees of freedom) is actually zero can be rejected at the 99% significance level; therefore, the amplitude of the continent-ocean geoid is (statistically) significant.
15. C. G. Chase and M. K. McNutt, *Geophys. Res. Lett.* **9**, 29 (1982).
16. M. A. Richards and B. H. Hager, *J. Geophys. Res.* **89**, 5987 (1984).
17. Y. Ricard, L. Fleitout, C. Froidevaux, *Ann. Geophys.* **2**, 267 (1984).
18. A. M. Forte and W. R. Peltier, *J. Geophys. Res.* **92**, 3645 (1987).
19. The gravitationally consistent calculation of viscous flow in a compressible mantle uses the formalism developed by A. M. Forte and W. R. Peltier [*ibid.* **96**, 20131 (1991)]. This viscous-flow calculation requires a model of the depth variation of mantle viscosity. The viscosity model we used (Fig. 1B) was obtained by slightly modifying a viscosity profile (*1*, *5*) inferred from nonhydrostatic geoid data. The modification consists of the introduction of a low-viscosity layer in the asthenosphere and a more strongly accentuated low-viscosity layer at the bottom of the mantle (in the so-called D″ layer). The viscosity model used here varies only with depth, and we thus ignored the effects of lateral viscosity variations, such as the possible (and likely) existence of a high-viscosity subcontinental mantle and a low-viscosity suboceanic mantle. A detailed investigation of mantle flow in the presence of such large-amplitude, large-scale lateral viscosity variations, by A. M. Forte and W. R. Peltier [*Adv. Geophys.* **36**, 1 (1994)] showed that their impact on predictions of surface topography and nonhydrostatic geoid is much smaller than the impact of changes in the depth variation of viscosity.
20. The cross-correlation between the correlated geoid and the geoid predicted on the basis of the uncorrelated seismic model $(\delta v_S/v_S)_{th}$ is only 0.16. This demonstrates that the origin of the continent-ocean geoid is indeed found in the density heterogeneity derived from the correlated seismic model $(\delta v_S/v_S)_{co}$.
21. S.-I. Karato, *Geophys. Res. Lett.* **20**, 1623 (1993).
22. The harmonic coefficient describing the ellipticity of the nonhydrostatic geoid predicted on the basis of the single density-velocity scaling (the short-dashed line in Fig. 1C, applied to both the correlated and the uncorrelated seismic models) is only −16 m. This prediction is considerably smaller than the precise satellite-derived value of −27.6 m, and, as pointed out in (*1*), this important discrepancy has been found on the basis of the use of other available seismic heterogeneity and mantle viscosity models.
23. T. H. Jordan, *Bull. Seismol. Soc. Am.* **71**, 1131 (1981).
24. The surface topography predicted with this stabilized continent-ocean density heterogeneity is characterized by an rms amplitude of about 0.5 km, with peak undulations of about 1 km (in the degree range ℓ = 1 to 8). We call this surface topography "quasi-isostatic" because the underlying continent-ocean density contrasts produce little vertical flow in the mantle (Fig. 2B). The surface topography predicted with the (thermal) density heterogeneity derived from the uncorrelated seismic model is characterized by an rms amplitude of about 0.8 km (in the degree range ℓ = 1 to 8), and we call it "dynamic" topography because the underlying density perturbations produce significant flow in the mantle (Fig. 2D). The total large-scale topography observed at Earth's surface is, in principle, the result of the superposition of (purely) isostatic topography due to compensated crustal heterogeneity and the quasi-isostatic and dynamic topographies considered here. The relative magnitudes of dynamic and isostatic topography have been the subject of recent debate [B. H. Hager, J. P. Grotzinger, S. S. Shapiro, S. V. Panasyuk, *Eos* (Spring Meeting Suppl.) **74**, 298 (1993); M. Gurnis, *Geophys. Res. Lett.* **20**, 1663 (1993); A. M. Forte, W. R. Peltier, A. M. Dziewonski, R. L. Woodward, *ibid.*, p. 1665]. The results reported here resolve much of these differences.
25. A. Chopelas and R. Boehler, *Geophys. Res. Lett.* **19**, 1983 (1992).
26. The temperature difference between average subcontinental mantle and average suboceanic mantle (denoted here by δT_{co}) can be estimated on the basis of the correlated seismic model $(\delta v_S/v_S)_{co}$ and the temperature derivative $\partial \ln v_S/\partial T$. An upper limit for this temperature contrast is obtained by calculating $\delta T_{co} = (\partial \ln v_S/\partial T)_{an}^{-1} (\delta v_S/v_S)_{co}$, in which $(\partial \ln v_S/\partial T)_{an}$ is a temperature derivative of seismic velocity due only to anharmonic effects [we are in effect assuming that the impact of seismic attenuation considered in (*21*) is less important in the cold mantle roots]. Here we used the anharmonic derivative measured by A. Chopelas [*Earth Planet. Sci. Lett.* **114**, 185 (1992)], and we thus estimated the following upper limits for continent-ocean temperature contrasts (the negative sign indicating that subcontinental mantle is colder than suboceanic mantle): $\delta T_{co} \approx -400$ K at a depth of 100 km, $\delta T_{co} \approx -200$ K at 400 km, and $\delta T_{co} \approx -50$ K at 600 km. These temperature contrasts are obtained on the basis of the complete continent-ocean function (synthesized from all harmonics). We also estimated relative density contrasts due only to continent-ocean chemical heterogeneity [denoted here by $(\delta\rho/\rho)_{chem}$] by calculating

$$(\delta\rho/\rho)_{chem} = [(\delta \ln \rho/\delta \ln v_S)_{co} - (\delta \ln \rho/\delta \ln v_S)_{an}](\delta v_S/v_S)_{co}$$

in which $(\delta \ln \rho/\delta \ln v_S)_{an} \approx 0.4$ is the anharmonic density-velocity scaling. We thereby obtained the following estimates (the negative sign indicating that the subcontinental mantle is intrinsically lighter than the suboceanic mantle): $(\delta\rho/\rho)_{chem} \approx -0.5\%$ at a depth of 100 km, $(\delta\rho/\rho)_{chem} \approx -0.7\%$ at 400 km, and $(\delta\rho/\rho)_{chem} \approx -0.2\%$ at 600 km.

27. We thank two anonymous reviewers for constructive comments. This study, initially begun while A.M.F. was at Harvard University, was supported by grants from the U.S. National Science Foundation. A.M.F. also thanks the Institut de Physique du Globe de Paris (IPGP) for its support. This is IPGP contribution number 1357.

29 August 1994; accepted 26 January 1995